



## Open Archive TOULOUSE Archive Ouverte (OATAO)

OATAO is an open access repository that collects the work of Toulouse researchers and makes it freely available over the web where possible.

This is an author-deposited version published in : <http://oatao.univ-toulouse.fr/>  
Eprints ID : 18233

**To link to this article** : DOI : 10.1117/12.2249994  
URL : <http://dx.doi.org/10.1117/12.2249994>

**To cite this version** : Cambouives, Adrien-Richard and Velluet, Marie-Thérèse and Poulenard, Sylvain and Saint-Antonin, Laurent and Michau, Vincent *Optical ground station optimization for future optical geostationary satellite feeder uplinks*. (2017) In: Photonics West 2017, 28 January 2017 - 2 February 2017 (San Francisco, United States).

Any correspondence concerning this service should be sent to the repository administrator: [staff-oatao@listes-diff.inp-toulouse.fr](mailto:staff-oatao@listes-diff.inp-toulouse.fr)

# Optical Ground Station optimization for future optical geostationary satellite feeder uplinks

A-R. Camboulives<sup>a,b</sup>, M-T. Velluet<sup>b</sup>, S. Poulenard<sup>c</sup>, L. Saint-Antonin<sup>a,c</sup>, V. Michau<sup>b</sup>

<sup>a</sup>IRT Saint-Exupery, 118 Route de Narbonne, Toulouse, France;

<sup>b</sup>ONERA-DOTA, 29 Avenue de la Division Leclerc, Châtillon, France;

<sup>c</sup>Airbus Defence and Space, 31 rue des cosmonautes, Toulouse, France

## ABSTRACT

An optical link based on a multiplex of wavelengths at 1.55  $\mu\text{m}$  is foreseen to be a valuable alternative to the conventional radio-frequencies for the feeder link of the next-generation of high throughput geostationary satellite. Considering the limited power of lasers envisioned for feeder links, the beam divergence has to be dramatically reduced. Consequently, the beam pointing becomes a key issue.

During its propagation between the ground station and a geostationary satellite, the optical beam is deflected (beam wandering), and possibly distorted (beam spreading), by atmospheric turbulence. It induces strong fluctuations of the detected telecom signal, thus increasing the bit error rate (BER). A steering mirror using a measurement from a beam coming from the satellite is used to pre-compensate the deflection. Because of the point-ahead angle between the downlink and the uplink, the turbulence effects experienced by both beams are slightly different, inducing an error in the correction.

This error is characterized as a function of the turbulence characteristics as well as of the terminal characteristics, such as the servo-loop bandwidth or the beam diameter, and is included in the link budget. From this result, it is possible to predict intensity fluctuations detected by the satellite statistically (mean intensity, scintillation index, probability of fade, etc.). The final objective is to optimize the different parameters of an optical ground station capable of mitigating the impact of atmospheric turbulence on the uplink in order to be compliant with the targeted capacity (1Terabit/s by 2025).

**Keywords:** Optical Communications, Atmospheric propagation, Tip/tilt correction

## 1. INTRODUCTION

An optical link based on a multiplex of wavelengths around the 1.55  $\mu\text{m}$  spectral band is foreseen to be a valuable alternative to the conventional radio-frequencies for the feeder links of next generation broadband geostationary satellites, targeting a capacity of around 1Tbps. In addition to cloud obstruction, one of the major limitations to optical links is the presence of atmospheric turbulence during the first 20 km of propagation. Atmospheric turbulence results in the presence of local fluctuations of the refractive index which deform the optical wave during its propagation. In this paper, we will focus on the uplink.

During its propagation from a ground station to a geostationary satellite, the optical beam is deflected (beam wandering), and possibly distorted (beam spreading), by atmospheric turbulence. It induces strong fluctuations of the detected telecommunication signal, thus increasing the Bit Error Rate (BER). To correct these effects, the beam characteristics need to be modified at the emission (pre-compensation). The envisaged technique is adaptive optics (AO) in which a servo system modifies in real time the emitted wavefront in order to make it recover a plane waveform when reaching the satellite. To do so, the beam coming from the satellite will be used to measure and estimate the perturbations that need to be applied to the emitted wavefront. Because of the point-ahead angle between the downlink and the uplink (due to the finite celerity of light), of the optical ground station architecture and of the delay between the measurement and the correction, the turbulence effects experienced by the downlink and the uplink are slightly different, leading to partial compensation only.

The objective of this paper is to present the results of a sensitivity study conducted to optimize an optical ground station architecture as a function of the propagation channel. This paper is organized as follows: In Section 2, we will present the different parameters we will take into account for the sensitivity study by describing

the optical ground station, the propagation channel and the criteria we will use to assess the system performance. In Section 3, we will present the model we use to simulate the results for the irradiance detected by the satellite. In Section 4, the optical link budgets at 5%-probability of the cumulative distribution function are derived as criteria of the sensitivity study. Finally, Section 5 concludes the paper by summarizing the important results for optical ground station sizing.

## 2. CONTEXT

### 2.1 Optical link budget

The optical link budget gives an estimation of the received power  $P_R$  as a function of the emitted power  $P_E$ , taking into account all losses  $L$  during the beam propagation :  $P_R = L_{TURB}L_{OTHERS}P_E$ , with  $L_{TURB}$ , losses induced by turbulence, and  $L_{OTHERS}$ , those induced by the other contributors. The emitter power considered equals 50 W. Atmospheric turbulence is a random phenomenon and thus implies that detected irradiance fluctuations are random as well. Therefore, a statistical approach will be considered, focusing on one quantity: the irradiance threshold  $I_T$  defined by  $P(I > I_T) = 0.95$ , where  $I$  is the instantaneous detected irradiance. Finding  $I_T$  provides the loss term  $L_{TURB}$  due to atmospheric turbulence at a 5%-probability of the cumulative distribution function. All the other quantities ( $L_{OTHERS}$ ) are set and static.

The optical receiver architecture is based on direct detection with On-Off-Keying modulation format. The optical receiver is on an Erbium Doped Fiber Amplifier (EDFA) followed by a PIN photodiode. The electrical noise after photodetection can be model by an asymmetrical Gaussian model. The model is asymmetric because the variance of electrical noise depends on the emitted bits being either '0' or '1'. These variances can be determined.<sup>1</sup> From these variances, the electrical signal-to-noise ratio (i.e. the Q-factor) can be derived as well as the Bit Error Rate (BER). It results that the optical power required for a 10Gbit/s link and a BER of 1E-3 is -43dBm.

### 2.2 Optical propagation channel characteristics

#### Description of the atmospheric turbulence

The air temperature fluctuations induce local refractive index variations which are neither constant nor homogeneous along the line of sight. Refractive index fluctuations are usually described through their power spectral density. Different models of power spectral densities exist. We assume a Von Kármán spectrum,<sup>2</sup> which takes into account limitations due to the inner scale  $l_0$  and outer scale  $L_0$ . The variability of the refractive index is estimated by the refractive index structure parameters  $C_n^2$  which corresponds to the variance of the refractive index between two points separated by one meter. This parameter characterizes the turbulence strength. The profile for  $C_n^2$  as a function of the altitude  $h$  usually used is the Hufnagel-Valley profile<sup>3</sup> defined by:

$$C_n^2(h) = 0.00594 \left( \frac{v}{27} \right)^2 (10^{-5}h)^{10} e^{-\frac{h}{1000}} + 2.7 \times 10^{-16} e^{-\frac{h}{1500}} + C_g e^{-\frac{h}{100}} \quad (1)$$

In this paper, we will take  $C_g = 5.4 \times 10^{-14} \text{ m}^{-\frac{2}{3}}$  and  $v = 21 \text{ m/s}$ , which is a strong turbulence case (corresponding to a median day) with a  $r_0$  calculated at Zenith equal to 10 cm for a 1.55  $\mu\text{m}$  wavelength. The elevation angle will be considered equal to 40°, making the effective  $r_0$  equal to 8 cm.

#### Description of the wind profile

The wind profile that will be used throughout this paper is the classical Bufton profile<sup>3</sup> in which the atmospheric layers move with a 5 m/s speed at ground level ( $S_G$ ) and with a 25 m/s speed ( $S_P$ ) at an altitude of 10 km ( $H_P$ ), described in Equation 2 (with  $W_P = 4800 \text{ m}$ ).

$$V(h) = S_G + S_P e^{-\left(\frac{h-H_P}{W_P}\right)^2} \quad (2)$$

## Outer scale

The outer scale  $L_0$  can be explained physically as the maximum size for a turbulent eddy. It can have a great impact on the pointing errors variance whereas the inner scale has nearly no impact and will be neglected. In our study, when not stated otherwise, we will consider an outer scale equal to 5 m, constant along the line of sight.

## 2.3 Optical ground station

The foreseen optical ground station will comprise a Gaussian laser beam of waist size  $w_0$  (and of diameter  $D_{beam} = 2w_0$ ) emitted through a telescope  $T_X$  with a pupil diameter  $D_{T_X}$ , which truncates the beam. Figure 1 describes the different parameters of the emitter:

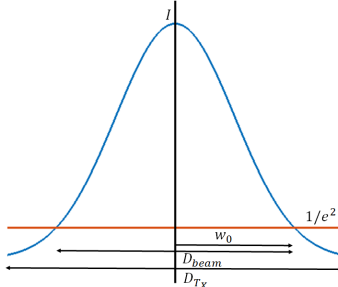


Figure 1: Description of the Gaussian beam parameters

Throughout this paper, the emitted Gaussian beam is considered collimated, i.e. that the position of the waist  $w_0$  is in the exit pupil of the emitter. Obscurations were not considered because adding one will modify the shape of the beam propagated throughout the atmosphere, which is not well documented.

The dimension of the beam waist is the first and principal parameter that will be studied. A small waist at the emission ( $w_0 \ll r_0$ ,  $r_0$  being the Fried parameter<sup>4</sup>) is less susceptible to the atmospheric turbulence effects but, due to the limited power of lasers envisioned for feeder links, the beam divergence has to be dramatically reduced (larger  $w_0$ , making the beam pointing a key issue. A trade-off will therefore have to be achieved, using a pointing error correction system, necessary to achieve the targeted power detected by the satellite.

Another parameter regarding the optical ground station that needs to be optimized is the diameter of the emission telescope. Indeed, because of the beam truncation by the telescope, diffraction will occur, reducing the mean detected irradiance and modifying the fluctuations. Moreover, the constraints of realizing an actual optical ground station impose a maximum size for the emission telescope. The maximum diameter considered for the telescope  $T_X$  is 50 cm.

Finally, the optical ground station will comprise an emitting telescope  $T_X$  and a receiving telescope  $R_X$  of diameter  $D_{R_X}$ . We assume that the phase measurement on the downlink will be made using a wavefront sensor of diameter  $D_{WFS}$  whose pupil is part of  $R_X$ .  $R_X$  and  $T_X$  may or may not be merged, depending on whether the possible stray light problems can be dealt with. Unless stated otherwise, we will consider that the pupil of the wavefront sensor is merged with the emitted beam.

## 3. TOOLS FOR MODELING IRRADIANCE IN THE SATELLITE PLANE

### 3.1 Statistical model for irradiance fluctuations

#### Model

The statistical model we use is derived from Baker's model.<sup>5</sup> It gives an estimation of the irradiance resulting from a Gaussian beam which moves in front of the satellite's detecting pupil. This model is very interesting because it takes into account the fact that the beam is slightly deformed because of defocus and astigmatism. However, it does not take into account the scintillation model<sup>6,7</sup> usually found in the literature in order to explain the irradiance fluctuations that are not due to beam wander.

We have refined it in order to take into account more parameters. With our improvements, we can take into account the effects of the outer scale and of the beam diffraction due to the finite size of the emitting telescope compared to the infinite Gaussian beam. This new model will be presented in detail in a future article.

With this model, through a Monte-Carlo method, we are able to generate very long sequences of random irradiances and, therefore, we are able to predict the irradiance fluctuations detected by the satellite statistically (mean irradiance, scintillation index, probability density function, probability of fade, etc.). We are then able to estimate the loss due to atmospheric turbulence at a 5%-probability of the cumulative density function.

### Validity domain of the model

This model relies on the fact that on a ground to space optical link, the irradiance is observed in the far-field of the beam while the perturbation due to atmospheric turbulence is located in the near field. It only gives results within the weak scintillation regime (i.e., the scintillation  $\sigma_I^2 < 1$ ) as it does not take into account the beam splitting phenomenon that appears in strong scintillation.

This model takes into account low orders of turbulence: tip/tilt errors, defocus and astigmatism. If we tolerate that the residual mean square phase errors between an exact solution and our model to be less than 0.1 wave squared (within a circle of radius  $w_0$ ), it can be shown that this gives the validity regime of the model:  $w_0 < 1.5r_0$ .

### 3.2 Correction of pointing errors

The idea behind pre-compensation is to inject the opposite of the Zernike tip/tilt coefficients ( $a_2/a_3$ ) measured on the downlink on the beam used for the uplink. The pointing error at the exit of the atmosphere is therefore:

$$a_{i,res}(t) = a_{i,U}(t) - a_{i,D}(t) \quad (3)$$

Where  $a_{i,res}$ ,  $a_{i,U}(t)$  and  $a_{i,D}(t)$  are respectively the residual tip/tilt error ( $i = 2, 3$ ), the tip/tilt on the uplink without pre-compensation and the tip/tilt measured on the downlink.

### Angular correlation of Zernike coefficients

The angular correlation gives an estimate of how much the fluctuations seen by the downlink resemble the fluctuations seen by the uplink. Its computation is based on F.Chassat's<sup>8</sup> work, which gives an estimation of the covariance of the tip and tilt (and of all the other Zernike polynomials) between two beams separated by an angle  $\alpha$ , corresponding to the point-ahead angle. As pointed out in Figure 2, the overlap of the two beams decreases with the altitude (as the distance  $d_{D \rightarrow U}(h)$  increases). The correlation between the tip ( $a_2$  within a circle of radius  $R_D(h)$ ) measured on the downwards propagating beam and the real tip on the upwards propagating beam (within a circle of radius  $R_U(h)$ ) is given by :

$$C = \frac{E[a_2 \cdot a_2(\alpha)]}{E[a_2^2]} \quad (4)$$

The correlation can never be greater than 1 and if it is inferior to 0.5, it means that correcting the uplink using the measurement from the downlink will add additional pointing errors and should therefore be avoided. This work also permits to estimate  $E[a_i^2]$ , which is the variance of the  $i^{th}$  Zernike polynomial. This variance can then be used to create random Zernike coefficients that can be incorporated in the model.

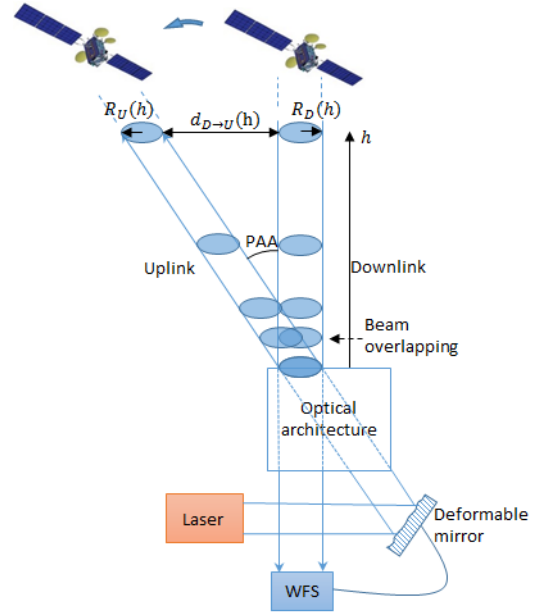


Figure 2: System architecture

Recently, Robert, Conan and Wolf<sup>9</sup> have shown that, by using the principle of reciprocity in propagation through turbulence, the upward propagation of a Gaussian beam can be modeled by the downward propagation of a plane wave. This result simplifies the estimation of the tip/tilt Zernike coefficients variance and of the correlation between the downlink and the uplink.

### Sources of residual pointing errors

In this study, only pointing errors (tip/tilt) will be corrected, which means that only a steering mirror will be used. The pointing errors cannot be perfectly corrected due to the fact that the downlink and the uplink do not overlap during their whole propagation through the atmosphere, as can be seen in Figure 2. The post-correction residual errors are a function of several parameters.

The first one is of course the point-ahead angle resulting from the finite celerity of light and from the Earth's rotation during the beam propagation. The point-ahead angle will be considered equal to  $18.5 \mu\text{rad}$  due to the fact that the optical ground stations will be placed in Europe.

Another source of error is the delay between the wavefront sensor measurement and the correction applied to the steering mirror. Throughout the study, a sampling frequency of 500 Hz and a 2 frames delay will be considered unless stated otherwise.

The spatial arrangement between the pupil of the wavefront sensor (WFS, with a diameter  $D_{WFS}$ ) and the emitting telescope diameter also has a great importance on the correction. Intuitively, an ideal case is where the pupil of the beam, of diameter  $D_{beam}$  (which is different from the telescope's  $D_{TX}$ ), and the pupil of the wavefront sensor  $D_{WFS}$  are superimposed. This will be confirmed during the sensitivity study. It will also be the reference case. In the case where such a system is not feasible, we will look into alternative architectures.

Finally, the vibrations of the station have been taken into account. They result in pointing errors that can be described by a Gaussian variable centered on a bias of  $1 \mu\text{rad}$  along the pointing direction and a standard deviation of  $0.2 \mu\text{rad}$  added to the pointing errors resulting from turbulence.

## 4. SENSITIVITY STUDY

The first part of the sensitivity study consists in optimizing the optical ground station architecture, studying the influence of the size of the waist at emission, of the beam truncation by the telescope, of the station vibrations, of the spatial arrangement between the emitted beam and the wavefront sensor, and of the sampling frequencies and delay times on the uplink budget. In the second part, the ground layer strength, the  $C_n^2$  profile and the outer scale are modified to evaluate the sensitivity of the system performance to these quantities. Throughout the study, we have made assumptions that the measurement of the Zernike coefficients on the downwards propagating beam by the system is perfect and that the correction will be perfectly applied to the upwards propagating beam.

### 4.1 Optical ground station

#### Waist

Figure 3 gives the evolution of the optical link budget as a function of the emitted waist size. Due to the model's validity regime, the waist sizes will range from 4 to 12cm. The effects of the truncation by the telescope and of the station's vibrations are not considered for now.

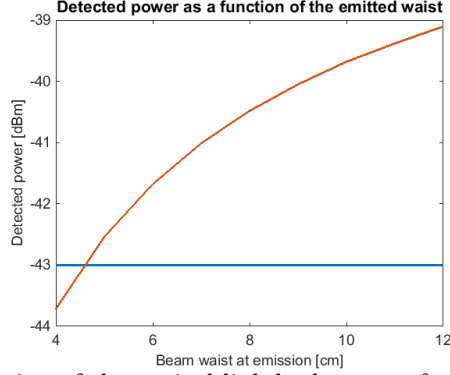


Figure 3: Evolution of the optical link budget as a function of the waist

Fulfilling the link budget is only possible for emitted beam waist sizes larger than 5 cm. The link budget is maximized for a waist of 12 cm. This is logical because the pointing errors are well corrected in the considered case (the tilt correlation between the downlink and the uplink is superior to 0.95 for a 12 cm waist at the emission) and therefore, a larger waist at the emission concentrates the energy on the satellite.

### Truncation ratio

We have studied the effects of the beam truncation for  $w_0 = 5$  cm,  $w_0 = 6$  cm,  $w_0 = 7$  cm, and  $w_0 = 12$  cm. Three different truncation ratios were taken into account :  $D_{T_x} = 2.1w_0$ ,  $D_{T_x} = 2^{\frac{3}{2}}w_0$  and  $D_{T_x} = 3w_0$ . The case without any truncation is taken as reference. The results expressed in dBm (optical link budget) are presented in Table 1:

		Optical link Budget [dBm]			
Truncation		$w_0 = 5$ cm	$w_0 = 6$ cm	$w_0 = 7$ cm	$w_0 = 12$ cm
$D_{T_x}$	$2.1w_0$	-44.77	-43.75	-42.96	-40.64
	$2^{\frac{3}{2}}w_0$	-43.11	-42.18	-41.47	-39.42
	$3w_0$	-42.95	-42.04	-41.34	-39.31
	No truncation	-42.54	-41.68	-41.01	-39.1

Table 1: Effects of the beam truncation on the budget link

Using a telescope diameter equal to  $D_{T_x} = 2.1w_0$  induces that fulfilling the link budget is only possible for emitted beam waist sizes larger than 7 cm. Using a telescope diameter  $D_{T_x} = 2^{\frac{3}{2}}w_0$  gives a good trade-off between optical link performance and telescope size, even though the minimum waist to fulfill the link budget becomes 6 cm. It is the truncation ratio that will be considered in the rest of the study.

### Optical Ground Station vibrations

The station vibrations are added to the study for waist sizes equal to  $w_0 = 5$  cm,  $w_0 = 6$  cm,  $w_0 = 7$  cm, and  $w_0 = 12$  cm. The telescope diameter is still equal to  $D_{T_x} = 2^{\frac{3}{2}}w_0$ . The results are presented in Table 2:

		Optical link Budget [dBm]			
		$w_0 = 5$ cm	$w_0 = 6$ cm	$w_0 = 7$ cm	$w_0 = 12$ cm
No vibrations		-43.11	-42.18	-41.47	-39.42
With vibrations		-43.2	-42.29	-41.6	-39.64

Table 2: Effects of the station vibrations on the budget link

The station vibrations add between 0.1 dB and 0.2 dB on the link budget. Their influence is therefore negligible.

### Sensor pupil and beam pupil arrangement

Here, we study the influence of the relative size diameter of the wavefront sensor and the emitter. Their axes are assumed to be aligned. In Figure 4, the result is given for a waist size  $w_0 = 12$  cm : These results are given for  $w_0 = 12$  cm :

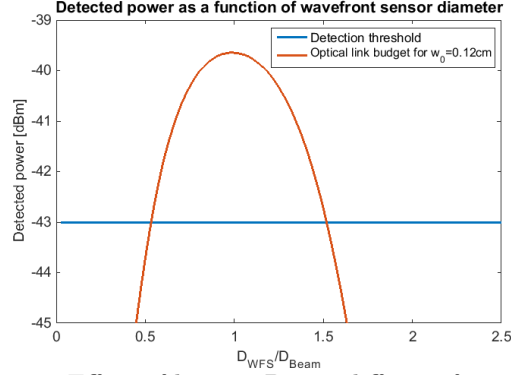


Figure 4: Effect of having  $D_{WFS}$  different from  $D_{beam}$

We see the importance of having  $D_{WFS}$  close to  $D_{beam}$  to have a functioning system. In order to lose less than 1 dB on the link budget,  $D_{WFS}$  should be between  $0.7D_{beam}$  and  $1.3D_{beam}$ . There is a 3 dB margin when  $D_{WFS}$  is equal to  $D_{beam}$ . This means that having a small difference between  $D_{WFS}$  and  $D_{beam}$  (inferior to 30% of  $D_{beam}$ ) is not problematic.

### Architecture

Up until now, we have assumed the pupil of the wavefront sensor was a part of the receiving telescope of diameter  $D_{R_X}$  and that the emitting telescope  $T_X$  was also a part of  $R_X$ . Alternative architectures are also envisioned in the case where it is impossible to use only one telescope for receiving the downlink and emitting the uplink because of stray light for example. The first alternative architecture looked into is the off-axis configuration (Figure 5a), where the pupil of the wavefront sensor is the receiving telescope and the emitting telescope is next to it. The second alternative architecture consists of having the telescopes in an annular configuration as shown in Figure 5b.

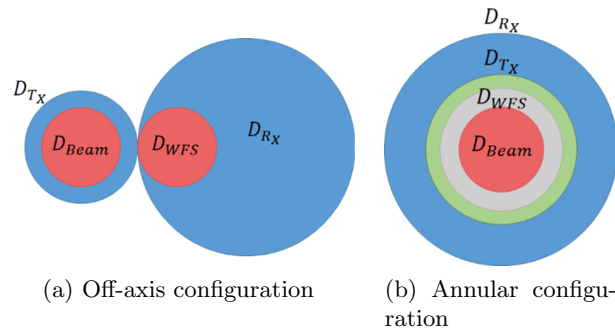


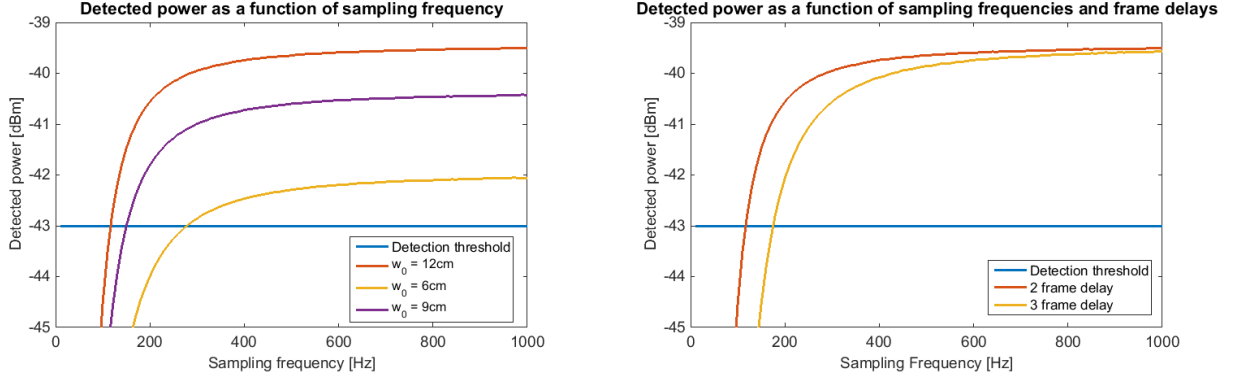
Figure 5: The two alternative architectures studied

With these architectures, it can be shown that the correction through pre-compensation never allows for improvement of the optical link budget because the correlation of the Zernike coefficients between the downlink and the uplink never increases above 0.5. This means that the wavefront measurement needs to be made on the same pupil as the emitted beam.



## Sampling frequencies and delay before correction

In Figure 6a, the evolution of the optical link budget is given as a function of the sampling frequency for  $w_0 = 6$  cm,  $w_0 = 9$  cm and  $w_0 = 12$  cm waists and a two frames delay (the sampling frequency is equal to the number of frames per second):



(a) Optical link budget as a function of sampling frequency with a 2 frame delay for 6cm, 9cm and 12cm waists. (b) Optical link budget as a function of sampling frequency with a 2 and 3 frame delay for a 12cm waist.

Figure 6: Sampling frequencies and frame delays studies

In Figure 6b, we present the evolution of the optical link budget is given as a function of the sampling frequency for a 12 cm waist with two or three frames delays. These results show that when the sampling frequencies are low, adding an additional frame before the correction adds a much longer delay and therefore significantly decreases the performance of the system. At constant number of delay frames, the optical link budget increases rapidly with the sampling frequency and then saturates. This shows that after a certain point, reducing the delay of correction does not significantly increase the performance. This is directly linked to the quality of the correction (therefore, to the correlation). These results also depend on the width of the beam and the average wind speed. We have found empirically that a good estimate of the minimum sampling frequency  $f_{sampling}$  for a specific number of delay frames  $N_{frames}$  is given by :

$$f_{sampling} = \frac{S_G N_{frames}}{0.5w_0}, \quad (5)$$

Where  $S_G$  is the speed of the wind at the ground layer level.

## 4.2 Optical channel of propagation

### Importance of the ground turbulence layer

Here, we study the influence of the turbulence strength near the ground, which can greatly fluctuate depending on whether it is day or night, on the season or on the localization of the station. We compare our reference model (described in Section 2.2) with a case where the value of  $C_n^2$  near the ground equals to  $1.7 \times 10^{-14} \text{ m}^{-2/3}$ , leading to a  $r_0 = 15$  cm at the given elevation (instead of 8 cm for the reference  $C_n^2$  profile) . The results are presented in Figure 7:

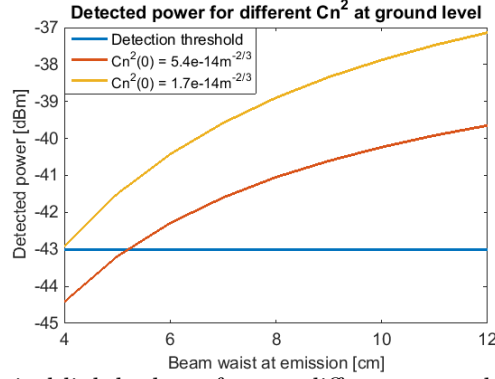


Figure 7: Optical link budgets for two different ground layer strengths.

The impact of the ground layer on the system link budget is quite important. The link budget improves by around 2 dB and the minimum waist size to fulfill the link budget becomes 4 cm.

### Modified $C_n^2$ profiles with stronger turbulence layers

Modified  $C_n^2$  profiles and resulting optical link budgets are plotted in Figure 8. The strength of the turbulence in the layers at 5 and 10 km is increased by approximately ten times compared to the reference model described in Section 2.2. Four different models were considered. The red profile has a peak at a 10 km height. The yellow profile has a peak at a 5 km height. The green profile has two peaks at 5 and 10 km heights. Finally, the violet profile has a peak at a 5 km height but the turbulence at the peak is three times stronger than for the other profiles. For all of these profiles,  $r_0$  is equal to 8 cm.

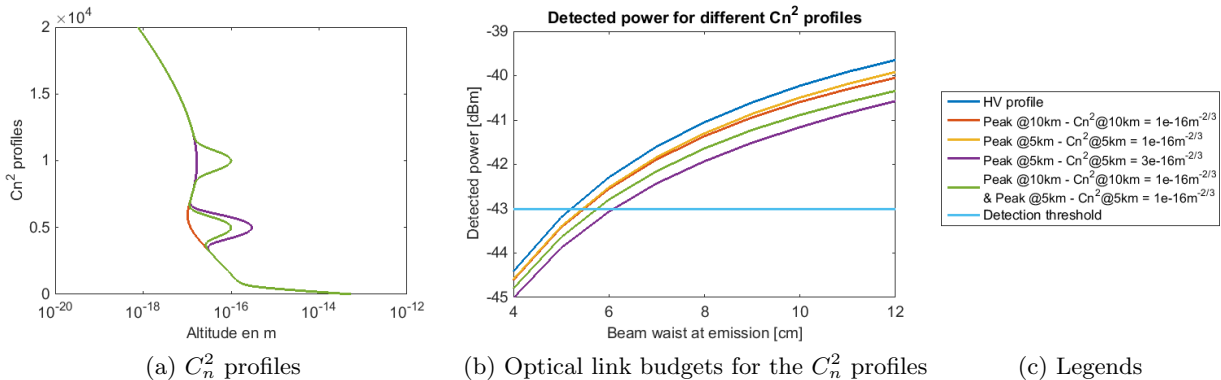


Figure 8: Comparison of the optical link budgets for different  $C_n^2$  profiles having stronger turbulence layers at high altitude

These results show that the loss in correlation due to the stronger turbulence layers induces some loss on the optical link budgets, but the loss is tolerable as inferior to 1 dB. The position of the layers has minor influence, as can be seen with the yellow and red curves. This shows that the beams are already uncorrelated at an altitude of 5 km. The worst results are obtained when there is a stronger peak at 5 km in altitude. When there are two peaks, both add their effects on the performance on the link. Finally, the increase of the high layer turbulence strength requires a bigger waist to fulfill the link budget.

### Outer scale

Finally, the effects of the outer scale on the optical link budget are evaluated. Without any correction, the outer scale plays a very important role on the pointing errors and a larger outer scale induces bigger pointing errors.

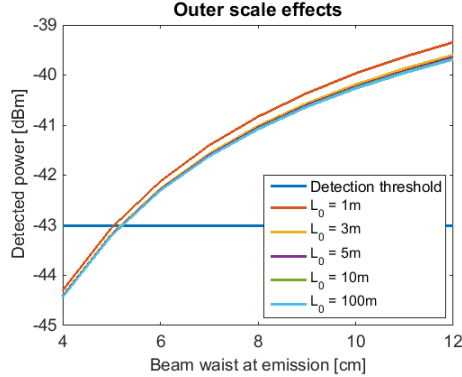


Figure 9: Optical link budgets for different outer scales.

However, after correction, we see that the influence of the outer scale is very small. For small outer scales such as 1 m, there is a small improvement on the uplink optical budget. However, there is almost no difference for outer scales bigger than 3 m. The criteria that can be used is the  $D_{beam}/L_0$  ratio. The outer scale has no influence when it is inferior to 0.1.

## 5. CONCLUSION

Using a model for irradiance as a function of the optical ground station architecture and propagation channel, we have been able to identify important results for the optimization of a ground to space telescope. In our sensitivity on the optical ground station architecture, we have shown that tip/tilt correction using a fine pointing mirror has been confirmed as mandatory in order to reach the necessary powers for a functioning system. Moreover, increasing the waist at the emission leads to better performance as long as the beam is not too deformed by atmospheric turbulence. The telescope truncation ratio induces some loss on the optical link budgets but with a sufficiently big telescope ( $D_{Tx} = 2^{3/2}w_0$  seems to provide a good trade-off between compactness and performance), the losses become negligible. The optical ground station vibrations have almost no impact on the optical link budget. The pupils of the beam and of the wavefront sensor need to be aligned in order to fulfill and maximize the optical link budget. This implies that there is work to be done on the optical architecture to avoid problems due to stray light because of the important power used for the uplink. Finally, we have proposed a simple equation to find the right combination of sampling frequencies and delay frames as a function of the size of the waist and the speed of the wind at the ground layer level.

In our sensitivity study on the optical channel of propagation, we have shown that the strength of the turbulence layer at ground level has an important impact on the link budget. Adding stronger turbulence layers at different altitudes induce losses on the optical link budget whereas the outer scale has almost no effect on the link budget.

In a future work, we will use this model to study the temporal fluctuations of intensity in order to be able to start sizing the error correcting codes.

## REFERENCES

- [1] Winzer, P. J., Kalmar, A., and Leeb, W. R., “Role of amplified spontaneous emission in optical free-space communication links with optical amplification: impact on isolation and data transmission and utilization for pointing, acquisition, and tracking,” (1999).
- [2] Tatarski, V., [*Wave Propagation in a Turbulent Medium*], Dover Publications Inc. (1961).
- [3] Hardy, J., [*Adaptive Optics for Astronomical Telescopes*], Oxford series in optical and imaging sciences, Oxford University Press (1998).
- [4] Fried, D., “Optical resolution through a randomly inhomogenous medium for very long and very short exposures,” *Journal of the Optical Society of America*, 1372–1379 (1966).

- [5] Baker, G. J., “Gaussian beam weak scintillation: low-order turbulence effects and applicability of the rytov method,” *J. Opt. Soc. Am. A* **23**, 395–417 (Feb 2006).
- [6] Andrews, L. C., Phillips, R. L., Sasiela, R. J., and Parenti, R. R., “Strehl ratio and scintillation theory for uplink gaussian-beam waves: beam wander effects,” *Optical Engineering* **45**(7), 076001–076001–12 (2006).
- [7] Dios, F., Rubio, J. A., Rodríguez, A., and Comerón, A., “Scintillation and beam-wander analysis in an optical ground station-satellite uplink,” *Appl. Opt.* **43**, 3866–3873 (Jul 2004).
- [8] Chassat, F., *Propagation optique à travers la turbulence atmosphérique : étude modale de l’anisoplanétisme et application à l’optique adaptative*, physique, Université Paris-Sud (June 1992).
- [9] Robert, C., Conan, J.-M., and Wolf, P., “Impact of turbulence on high-precision ground-satellite frequency transfer with two-way coherent optical links,” *Phys. Rev. A* **93**, 033860 (Mar 2016).